THE DISSIPATION AND DISPERSION OF SMALL WAVES IN ARTERIES AND VEINS WITH VISCOELASTIC WALL PROPERTIES

JAMES A. MAXWELL *and* MAX ANLIKER

From the Department of Aeronautics and Astronautics, Stanford University, Stanford, California 94305

ABSTRACT Theoretical and experimental evidence suggests that the dissipation of high frequency pressure waves in blood vessels is caused primarily by the viscoelastic behavior of the vessel wall. In this theoretical analysis the vessels are considered as fluid-filled circular cylindrical shells whose walls have isotropic and homogeneous viscoelastic properties and are subjected to an initial axial stretch and a transmural pressure. If the wall material is incompressible and behaves as a Voigt solid in shear, the results predict a decrease in wave amplitude per wavelength which is essentially independent of frequency over a wide range. This finding is in qualitative agreement with recent experiments on anesthetized dogs. A parametric study also shows a great sensitivity of the dissipation to changes in transmural pressure and axial stretch. Axisymmetric waves are only mildly dispersive, while all nonaxisymmetric waves are highly dispersive and exhibit much stronger damping per wavelength at low frequencies than do axisymmetric waves.

INTRODUCTION

The transmission and generation of sounds and pulse waves within the cardiovascular system are phenomena of great importance in the diagnosis of circulatory disorders. These phenomena are utilized mostly on an empirical basis since we lack a satisfactory quantitative understanding of the mechanical behavior of the circulatory system. A reliable interpretation of sound generation and wave transmission data calls for mathematical models of the cardiovascular system or components thereof that have been validated by carefully planned experiments. A further incentive to study these phenomena from the physical sciences point of view is their usefulness in determining the elastic properties of arteries and veins and the changes of these properties under physical and physiological stresses that may for example be produced by trauma, prolonged weightlessness, or acceleration. The proper elastic behavior of blood vessels in situations of stress is essential to maintaining adequate circulation and is governed by intricate control mechanisms that are not yet fully understood.

The work presented here is part of a continued systematic study of the effects of various parameters and properties of the cardiovascular system on the transmission characteristics of sounds and pressure pulses. While this paper is of a theoretical nature, it makes use of recent results obtained from experimental investigations of the dispersion and dissipation of small sinusoidal pressure waves in various large vessels of anesthetized dogs. It differs from earlier analytical efforts reviewed or described in references 1 to 7 in the selection of the mathematical model for the dynamic behavior of the blood vessels. We assume the vessels to behave like circular cylindrical shells filled with an inviscid compressible fluid and having walls with isotropic and homogeneous viscoelastic properties. The waves are described by small three-dimensional sinusoidal displacements of the middle surface of the shell that are measured from an equilibrium configuration defined by a mean transmural pressure and an initial axial strain. The fluid motion associated with the waves is considered as irrotational and the displacement of the wall assumed to be governed by the shell equations derived by Flügge (8). We disregard the effect of a surrounding medium in this study, even though it may not be negligible in many cases. We also neglect the influence of the viscosity of the blood which has been studied by several investigators (3, 4, 6, 9) for certain types of waves. As such the mathematical model defined by these assumptions is similar to that used by the authors in an earlier study (10) except that now the vessel wall is viscoelastic rather than purely elastic.

As in reference 10, we include again in our consideration waves which exhibit a circumferential dependence of the corresponding displacements of the vessel wall. For each circumferential wave number, we also find in the viscoelastic case infinitely many waves with individual speeds of propagation, of which only the three slowest waves are not due to the compressibility of the fluid. In this investigation we shall again disregard all but the three slowest waves and denote these as waves of type I, II, and III. In waves of type I the radial displacement component is dominant at high frequencies, while in waves of type II, the circumferential, and in waves of type III, the axial displacement component dominates at high frequencies. Of these three types of waves, those of type II and III are less important from the practical point of view, since only type I waves have associated with themselves substantial fluctuations in fluid pressure.

From experimental evidence we know that the propagation of sounds and pulse waves within the cardiovascular system is subject to strong dissipative mechanisms. The dissipation of waves in blood vessels can be attributed to three main causes: viscosity of the blood, viscoelastic behavior of the wall, and radiation of energy into the surrounding medium. Some data on the combined effect of the various dissipative mechanisms in arteries under in-vivo conditions have been obtained by means of an indirect technique making use of simultaneous recordings of the natural pulse wave at various points along the aorta and other arteries of anesthe-

tized dogs. The data take into account the effects of reflections and dispersion and are based on the debatable assumption that the propagation of pressure pulses generated by the heart is governed by linear laws that permit a harmonic analysis.

The combined effect of the three main causes for dissipation has also been measured directly by a recently developed method based on artificially induced perturbations in the form of trains of sinusoidal pressure waves. This direct method has been applied to the thoracic and abdominal aorta and the inferior vena cava of anesthetized dogs (11). The results obtained with it reveal a strong frequency dependence of the dissipation per cm at frequencies between 12 and 200 cps while the dissipation per wavelength is essentially independent of frequency within this range. The dissipation per cm of the artificially induced sine waves exceeds by far the value that could be attributed to the viscosity of the blood alone (12, 13). Considering in addition that the dissipation of waves in the major vessels examined so far is essentially the same when the vessels are exposed, we conclude that at higher frequencies the primary cause for the attenuation must be the viscoelastic behavior of the vessel walls.

Several mathematical models have been postulated for dissipative mechanisms (3, 4, 6, 9, 14–16, 12) which take into consideration the viscosity of the fluid and/or viscoelastic properties of the vessel wall, but which largely adhere to a membrane analysis and exclusively consider only axisymmetric waves. Also, these models, with the exception of that of reference 9, have neglected the presence of an axial stretch and a transmural pressure. In our parametric study of dissipation and dispersion we are considering axisymmetric as well as nonaxisymmetric waves and include the effects of an axial stretch and a transmural pressure.

BASIC EQUATIONS

The signals considered are defined by the displacement components u, v, w of an arbitrary point of the middle surface of the vessel in the axial, circumferential, and radial direction, respectively. As illustrated in Fig. 1, the vessel is referred to a set of cylindrical coordinates x, r, β such that $r = a$ represents the middle surface of the vessel wall. In this analysis we take into account the fact that blood vessels are subjected to an initial axial stretch and a transmural pressure Δp. After application of the initial axial stretch the ends of the vessel are assumed to be fixed. We interpret $r = a$ as the unperturbed equilibrium configuration of the middle surface in the presence of a stationary axial stretch and a mean transmural pressure Δp. The parameters u, v, w are thus interpreted as displacement components measured from the equilibrium configuration. They are functions of the two coordinates x and β, implying that the waves to be studied are two-dimensional in character.

In order to derive the differential equations of motion for the viscoelastic vessel wall, we first consider the wall material to be elastic and then make use of the Correspondence Principle. Accordingly we first assume the vessel to behave like

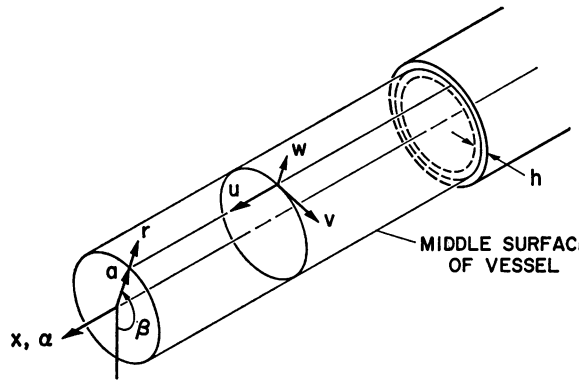

FIGURE 1 Coordinate system.

an elastic, homogeneous, isotropic and thin-walled circular cylindrical shell. Its wall thickness is denoted by h, its Young's modulus by E, and its Poisson's ratio by ν. The axial stretch of the vessel gives rise to an initial axial tension T_{10}. In the presence of an external pressure p_e, the transmural pressure Δp is given by

$$\Delta p = p_{io} - p_e \tag{1}$$

where p_{io} is the internal fluid pressure in the absence of any disturbances.

For convenience we introduce the dimensionless stress resultants in the axial and circumferential directions

$$q_1 = \frac{T_{10}(1 - \nu^2)}{Eh}, \tag{2}$$

$$q_2 = \frac{a\Delta p(1 - \nu^2)}{Eh} \tag{3}$$

and the two-dimensional Laplacian operator

$$\nabla^2 = \frac{\partial^2}{\partial\alpha^2} + \frac{\partial^2}{\partial\beta^2} \tag{4}$$

in which the nondimensional axial coordinate α is defined by

$$\alpha = \frac{x}{a}. \tag{5}$$

The elastic behavior of the vessel wall is assumed to be governed by the linearized equations for circular cylindrical shells derived by W. Flügge (8) which have been

shown to be useful also in analyzing the vibrations of cylindrical shells that can no longer be considered as thin-walled (17). Hence for small displacements from the equilibrium configuration and for shells whose length remains unchanged after the initial axial stretch has been applied we have the following differential equations for the displacement components u, v, w:

$$L_{11}(u) + L_{12}(v) + L_{13}(w) + (q_1 + \nu q_2)\frac{\partial^2 u}{\partial \alpha^2} + q_2\left(\frac{\partial^2 u}{\partial \beta^2} - \frac{\partial w}{\partial \alpha}\right) - \mu_w \frac{\partial^2 u}{\partial t^2} = 0,$$

$$L_{21}(u) + L_{22}(v) + L_{23}(w) + (q_1 + \nu q_2)\frac{\partial^2 v}{\partial \alpha^2} + q_2\left(\frac{\partial^2 v}{\partial \beta^2} + \frac{\partial w}{\partial \beta}\right) - \mu_w \frac{\partial^2 v}{\partial t^2} = 0,$$

$$L_{31}(u) + L_{32}(v) + L_{33}(w) - (q_1 + \nu q_2)\frac{\partial^2 w}{\partial \alpha^2} - q_2\left(\frac{\partial u}{\partial \alpha} - \frac{\partial v}{\partial \beta} + \frac{\partial^2 w}{\partial \beta^2}\right) + (\mu_w + \mu_f)\frac{\partial^2 w}{\partial t^2} = 0. \quad (6)$$

The differential operators L_{ij} are defined as

$$L_{11} = \frac{\partial^2}{\partial \alpha^2} + \frac{(1-\nu)}{2}\frac{\partial^2}{\partial \beta^2}(1 + e^2)$$

$$L_{22} = \frac{\partial^2}{\partial \beta^2} + \frac{(1-\nu)}{2}\frac{\partial^2}{\partial \alpha^2}(1 + e^2)$$

$$L_{33} = 1 + e^2\left(\nabla^2\nabla^2 + 2\frac{\partial^2}{\partial \beta^2} + 1\right)$$

$$L_{12} = L_{21} = \frac{(1+\nu)}{2}\frac{\partial^2}{\partial \alpha\, \partial \beta}$$

$$L_{13} = L_{31} = \nu\frac{\partial}{\partial \alpha} - e^2\left(\frac{\partial^3}{\partial \alpha^3} - \frac{(1-\nu)}{2}\frac{\partial^3}{\partial \alpha\, \partial \beta^2}\right)$$

$$L_{23} = L_{32} = \frac{\partial}{\partial \beta} - e^2\left(\frac{3-\nu}{2}\right)\frac{\partial^3}{\partial \alpha^2 \partial \beta} \quad (7)$$

where

$$e^2 = \frac{h^2}{12a^2}. \quad (8)$$

The quantities μ_w and μ_f are inertia parameters associated with the wall and the fluid and can be written in the form

$$\mu_w = \frac{(1 - \nu^2)}{Eh} a^2(\rho_w h) \tag{9}$$

$$\mu_f = \frac{(1 - \nu^2)}{Eh} a^2 m_f \tag{10}$$

where m_f denotes the apparent mass of the fluid and is defined by the perturbation pressure at the vessel wall as will be shown later.

The fluid contained within the vessel is assumed to be compressible and inviscid. Besides this we assume that the flow associated with the signals is irrotational and that the effects of a mean flow and of gravity can be neglected. The fluid velocity $\mathbf{v}$ is then given by

$$\mathbf{v} = -\nabla\Phi, \tag{11}$$

with ∇ denoting the three-dimensional gradient operator. Within the realm of a linearized theory the velocity potential Φ satisfies the three-dimensional continuity equation

$$\frac{1}{c_f^2}\frac{\partial^2\Phi}{\partial t^2} = \frac{\partial^2\Phi}{\partial x^2} + \frac{1}{r^2}\frac{\partial^2\Phi}{\partial\beta^2} + \frac{1}{r}\frac{\partial}{\partial r}\left(r\frac{\partial\Phi}{\partial r}\right) \tag{12}$$

with c_f denoting the speed of sound in the fluid. If p_i represents the perturbed intra-arterial pressure, p_{io} the internal pressure in the absence of a signal and ρ_f the fluid density, the linearized Euler equation can be written in the form

$$p_i = \rho_f \frac{\partial\Phi}{\partial t} + p_{io}. \tag{13}$$

The velocity potential Φ and the radial displacement component w are interconnected through the kinematic boundary condition

$$\frac{\partial w}{\partial t} = -\left(\frac{\partial\Phi}{\partial r}\right)_{r=a}. \tag{14}$$

As solutions to the continuity equation (12) we have

$$\Phi_{sk} = D_{sk} I_s\left(\xi\frac{r}{a}\right)\exp\left[i(kx - \omega t + s\beta)\right] \tag{15}$$

where D_{sk} is an amplitude defined by initial conditions, s is the circumferential wave number, ω the circular frequency, k the axial wave number, I_s the modified

Bessel function of the first kind of order s, and

$$\xi = \left(k^2a^2 - \frac{\omega^2a^2}{c_f^2}\right)^{1/2}. \tag{16}$$

The apparent mass m_f can be expressed in terms of the wall displacements that characterize the waves to be studied. To this end we utilize the relationship between the apparent mass and the pressure perturbation which in the case of inviscid irrotational flow can be written as

$$-m_f \frac{\partial^2 w}{\partial t^2} = (p_i - p_{io})_{r=a}. \tag{17}$$

Substituting from the linearized Euler equation (13) we obtain

$$-m_f \frac{\partial^2 w}{\partial t^2} = \rho_f \left(\frac{\partial \Phi}{\partial t}\right)_{r=a}. \tag{18}$$

We now assume as solutions to the differential equations (6) expressions that represent small sinusoidal waves propagating in the direction of the cylinder axis:

$$\begin{aligned} u &= A_{sk} \exp\left[i(kx - \omega t + s\beta)\right] \\ v &= B_{sk} \exp\left[i(kx - \omega t + s\beta)\right] \\ w &= C_{sk} \exp\left[i\left(kx - \omega t + s\beta + \frac{\pi}{2}\right)\right]. \end{aligned} \tag{19}$$

Combining equations 14, 15, 17, and 18, we find for the apparent mass

$$m_f = \rho_f a \frac{I_s(\xi)}{\xi I'_s(\xi)}. \tag{20}$$

The substitution of equation 19 into 6 leads to a set of three linear homogeneous equations for the coefficients A_{sk}, B_{sk}, and C_{sk}. Requiring that nontrivial solutions exist for A_{sk}, B_{sk}, and C_{sk}, we arrive at the frequency equation of the system.

To reduce the frequency equation to a convenient form we introduce the following dimensionless parameters:

$$\begin{aligned} &c_p^2 = E/[\rho_w(1 - \nu^2)], \quad \bar{c}^2 = c^2/c_p^2, \quad \bar{\omega}^2 = \omega^2a^2/c_p^2, \quad \bar{\rho} = \rho_f/\rho_w, \\ &c^{*^2} = c_f^2/c_p^2. \end{aligned} \tag{21}$$

Then

$$\xi = \frac{\bar{\omega}}{\bar{c}}\left(1 - \frac{\bar{c}^2}{c^{*2}}\right)^{1/2} \tag{22}$$

and the frequency equation can be written as

$$\begin{vmatrix} \frac{\bar{\omega}^2}{\bar{c}^2}(1+q_1+\nu q_2) & -\frac{(1+\nu)}{2}\frac{\bar{\omega}}{\bar{c}}s & \frac{\bar{\omega}}{\bar{c}}(\nu-q_2)+e^2\left[\frac{\bar{\omega}^3}{\bar{c}^3}\right. \\ +q_2 s^2+\frac{(1-\nu)}{2}s^2 & & \left.-\frac{(1-\nu)}{2}\frac{\bar{\omega}}{\bar{c}}s^2\right]. \\ \cdot(1+e^2)-\bar{\omega}^2 & & \\ & \frac{\bar{\omega}^2}{\bar{c}^2}\left[(q_1+\nu q_2)\right. & -e^2\frac{(3-\nu)}{2}\frac{\bar{\omega}^2}{\bar{c}^2}s \\ & \left.+\frac{(1-\nu)}{2}(1+3e^2)\right] & -(1+q_2)s \\ \text{SYMMETRIC} & +(1+q_2)s^2-\bar{\omega}^2 & \\ & & 1+e^2\left[\left(\frac{\bar{\omega}^2}{\bar{c}^2}+s^2\right)^2\right. \\ & & \left.-2s^2+1\right]+\frac{\bar{\omega}^2}{\bar{c}^2}(q_1 \\ & & +\nu q_2)+q_2 s^2 \\ & & -\left[1+\bar{\rho}\frac{a}{h}\frac{I_s(\xi)}{\xi I'_s(\xi)}\right]\bar{\omega}^2 \end{vmatrix} = 0 \tag{23}$$

VISCOELASTIC SHELL EQUATIONS

In the three-dimensional theory of linear viscoelasticity, an isotropic viscoelastic material is described by means of relationships specifying the material's behavior in shear and in dilatation; i.e.,

$$P(\tau_{ij}) = Q(\gamma_{ij}) \qquad i,j = 1,2,3; \quad i \neq j \tag{24}$$

and

$$\tfrac{1}{3}P'(\sigma_{ii}) = Q'(\epsilon_{ii}) \tag{25}$$

where P, Q, P', and Q' are linear differential operators of the form

$$L(D) = a_0 + a_1 D + a_2 D^2 + \cdots + a_n D^n \tag{26}$$

with $D \equiv \partial/\partial t$. The coefficients a_i are constants, and the operators P and Q may be chosen independent of P' and Q'. The viscoelastic equations are analogous to the elastic relations

$$\tau_{ij} = G(\gamma_{ij}) \qquad i,j = 1,2,3; \quad i \neq j \tag{27}$$

and

$$\tfrac{1}{3}\sigma_{ii} = K\epsilon_{ii} \tag{28}$$

in which G and K are the shear modulus and bulk modulus, respectively. From the elastic relationships

$$G = \frac{E}{2(1+\nu)}, \qquad K = \frac{E}{3(1-2\nu)} \tag{29}$$

and from the formal equivalences

$$Q/P = \tilde{G}, \qquad Q'/P' = \tilde{K} \tag{30}$$

one may, by algebraic manipulations, define operators $\tilde{E}$ and $\tilde{\nu}$ in terms of the viscoelastic operators P, Q, P', and Q'. One obtains

$$\tilde{E} = \frac{9QQ'}{3Q'P + QP'} \tag{31}$$

and

$$\tilde{\nu} = \frac{3Q'P - 2QP'}{2(3Q'P + QP')}. \tag{32}$$

Replacing the Young's modulus E, and Poisson's ratio ν, in the differential equations of motion for the fluid-filled elastic vessel (equations 6 and 7) by the operators $\tilde{E}$ and $\tilde{\nu}$ as defined by equations 31 and 32, one arrives at the differential equations of motion corresponding to a linearly viscoelastic vessel wall. The fluid equations of motion and kinematic boundary conditions are clearly unaffected by the assumptions made on the vessel wall material, so that the apparent mass term remains unchanged.

By substituting the trial solution (equation 19) into the differential equations of motion we obtain the frequency equation for the viscoelastic case, in which the wave number k must have a positive imaginary part if attenuation is to be present. To allow for a convenient description we write $k = k_R + ik_I$. The phase velocity of signals with an angular frequency ω is then given by $c = \omega/k_R$, while the signal is attenuated by a factor of exp $(-k_I x)$ after travelling a distance x.

It should be noted that for the trial solution (equation 19), the frequency equation can be obtained by formally substituting $-i\omega$ for D in the operators $\tilde{E}$ and $\tilde{\nu}$ given by equations 31 and 32 and by replacing E and ν in the elastic frequency equation (23) by $\tilde{E}$ and $\tilde{\nu}$. The viscoelastic parameters corresponding to E and ν will be complex, and for the sake of clarity, they will be denoted $\hat{E}$ and $\hat{\nu}$, respectively:

$$\hat{E} = \frac{9\hat{Q}\hat{Q}'}{3\hat{Q}'\hat{P} + \hat{Q}\hat{P}'} \tag{33}$$

$$\nu = \frac{3\hat{Q}'\hat{P} - 2\hat{Q}\hat{P}'}{2(3\hat{Q}'\hat{P} + \hat{Q}\hat{P}')} \tag{34}$$

with

$$\hat{P}(\omega) \equiv (P)_{D\to -i\omega} \quad \hat{Q}(\omega) \equiv (Q)_{D\to -i\omega} \quad \hat{P}'(\omega) \equiv (P')_{D\to -i\omega} \quad \hat{Q}'(\omega) \equiv (Q')_{D\to -i\omega}. \tag{35}$$

VISCOELASTIC MODELS

In one-dimensional linear viscoelasticity it is convenient to interpret expressions of the form $P\sigma = Q\epsilon$ as a mathematical model of a mechanical system consisting of springs and dashpots. Because of mathematical complexities, this mechanical system is usually restricted to three simple models: the standard linear solid, the Maxwell fluid, and the Voigt solid. In the three-dimensional case the problem may become completely intractable when independent models for both the shear and dilatational behavior of the material must be selected. A major simplification can be achieved if the material is assumed to be incompressible. Utilizing the fact that most biological materials, including blood vessels, are nearly incompressible, we assume that

$$\frac{\hat{P}'}{\hat{Q}'} = 0. \tag{36}$$

From this it follows that

$$\hat{E} = 3\hat{Q}/\hat{P} \tag{37}$$

and

$$\nu = \tfrac{1}{2}. \tag{38}$$

Thus the viscoelastic properties of the material are now completely determined by its behavior in shear and a single viscoelastic model suffices to characterize the stress-strain laws of the material. In the case of the three simple models mentioned above, $\hat{E}$ becomes:

$$\begin{aligned} &\text{Standard linear solid} && \hat{E} = \frac{E_1 E_2}{E_1 + E_2}\,\frac{1 - i\eta\omega/E_2}{1 - i\eta\omega/(E_1 + E_2)} \\ &\text{Maxwell fluid} && \hat{E} = \frac{-3i\eta\omega}{(1 - i\eta\omega/E_0)} \\ &\text{Voigt solid} && \hat{E} = 3(E_0 - i\eta\omega). \end{aligned} \tag{39}$$

Irrespective of the viscoelastic behavior, $\hat{E}$ may be written in the form

$$\hat{E} = \hat{E}_R(\omega) + i\hat{E}_I(\omega). \tag{40}$$

In fact, equations 38 and 40 may be taken as the starting point for an analysis of waves in a viscoelastic vessel, with the functions $\hat{E}_R(\omega)$ and $\hat{E}_I(\omega)$ selected so as to exhibit certain properties determined from experimental data. Such an approach has been employed in references 15 and 16. However, these investigations have been restricted to axisymmetric vibrations using an unrealistic mechanical model for the vessel, since initial axial stretch and a transmural pressure were neglected. Of interest is a systematic analysis of the effects of a viscoelastic behavior of the vessel wall including the influence of initial loading, bending rigidity, and also allowing for nonsymmetrical waves.

Of the three simple viscoelastic models considered here, it is clear that the standard linear solid allows for the most complete representation of the viscoelastic behavior of blood vessels, since it includes the Maxwell fluid and Voigt solid as special cases. However, three independent parameters must be selected to define such a solid, while only two are needed for the Maxwell or Voigt model. For a thorough parametric analysis, the computational effort increases considerably with each additional parameter. Therefore, attention will be restricted to the Maxwell and Voigt models.

The decision as to whether the Maxwell or Voigt model is the more appropriate must be made on the basis of experimental evidence. Results of recent experiments (11) indicate that in the range from 50 to 200 cycles per sec the damping per wavelength of type I waves in the thoracic aorta of anesthetized dogs is essentially independent of frequency. Assuming, as a first approximation, that the phase velocity c of type I waves is given by the Moens-Korteweg formula

$$c^2 = \frac{Eh}{2\rho_f a}$$

for all frequencies, it follows that in the viscoelastic case, the damping per wavelength for the Voigt model in shear is given by

$$\frac{A_\lambda}{A_0} = \exp\left\{-2\pi\left[\frac{(1 + 3\hat{\eta}^2\hat{\omega}^2)^{1/2} - 1}{(1 + 3\hat{\eta}^2\hat{\omega}^2)^{1/2} + 1}\right]^{1/2}\right\} \tag{41}$$

while the Maxwell model yields

$$\frac{A_\lambda}{A_0} = \exp\left\{-2\pi\left[\frac{(1 + 1/3\hat{\eta}^2\hat{\omega}^2)^{1/2} - 1}{(1 + 1/3\hat{\eta}^2\hat{\omega}^2)^{1/2} + 1}\right]^{1/2}\right\}. \tag{42}$$

In these expressions A_0 and A_λ are the wave amplitudes at $x = 0$ and $x = \lambda$, respectively, with λ denoting the wavelength. For large $\hat{\omega}$, A_λ/A_0 approaches exp (-2π) for the Voigt model and 1.0 for the Maxwell model. From this we conclude that at high frequencies, the Maxwell model predicts an extremely small attenuation which is in contrast with experimental observations. It should be noted that

the phase velocity c and A_λ/A_0 have also been determined by solving the frequency equation for the viscoelastic shell using the Maxwell model. The results again show that the Maxwell model does not lead to damping characteristics and phase velocities which are in agreement with experimental evidence. On the other hand, as will be shown, the Voigt model reflects more realistic wave propagation characteristics. We have therefore restricted our parametric study of wave propagation to blood vessels whose shear deformation is governed by a Voigt model.

NORMALIZATION

In the elastic case we introduced as normalizing velocity

$$c_p = \left[\frac{E}{\rho_w(1 - \nu^2)}\right]^{1/2}. \tag{43}$$

Since, for viscoelastic material $\hat{E}$ and $\hat{\nu}$ are in general both complex functions of frequency, the above expression for c_p would lead to a complex velocity. We avoid this by introducing in lieu of the above definition a normalizing velocity

$$c_b = \left[\frac{\hat{E}_0}{\rho_w}\right]^{1/2} \tag{44}$$

where $\hat{E}_0$ is real and is equal to the value of the complex Young's modulus $\hat{E}$ taken for $\omega = 0$. In particular, for the Voigt model we have

$$c_b = \left[\frac{3E_0}{\rho_w}\right]^{1/2} \tag{45}$$

We additionally introduce the following dimensionless parameters:

$$\begin{aligned}
\hat{c}^2 &= c^2/c_b^2 \\
\hat{\omega}^2 &= \omega^2 a^2/c_b^2 \\
\hat{c}^{*2} &= c_f^2/c_b^2 \\
\hat{q}_1 &= T_{10}/3E_0h \\
\hat{q}_2 &= a\Delta p/3E_0h \\
\hat{\eta} &= \eta/[a\rho_w(E_0/\rho_w)^{1/2}].
\end{aligned} \tag{46}$$

It is interesting to note that in the expression for $\hat{\eta}$, the quantity $(E_0/\rho_w)^{1/2}$ has the dimension of a speed. Hence, $1/\hat{\eta}$ may be considered to be a viscoelastic Reynolds number, in which the tube radius a is the characteristic length and $(E_0/\rho_w)^{1/2}$ the characteristic speed.

RESULTS OF VISCOELASTIC SHELL ANALYSIS

The frequency equation for the viscoelastic case interrelates eleven dimensionless parameters $\hat{\nu}$, s, h/a, $\bar{\rho}$, $\hat{q}_1$, $\hat{q}_2$, $\hat{\omega}$, $\hat{c}$, $\hat{c}^*$, $k_I a$, and $\hat{\eta}$. The first nine parameters are basically the same as in the elastic case, except that the five parameters $\hat{q}_1$, $\hat{q}_2$, $\hat{\omega}$, $\hat{c}$, and $\hat{c}^*$ differ by constant factors from q_1, q_2, $\bar{\omega}$, $\bar{c}$, and $\bar{c}^*$. In addition to these first nine parameters we now have also a measure of the wave attenuation in the form of $k_I a$, the imaginary part of the complex wave number, and the dimensionless coefficient of viscosity $\hat{\eta}$. It is convenient and more descriptive to present the effects of damping in the form of the amplitude ratio A_λ/A_0 in lieu of $k_I a$. From equation 19 it follows immediately that A_λ/A_0 is given by

$$A_\lambda/A_0 = \exp\left[-2\pi \frac{k_I}{k_R}\right]. \tag{47}$$

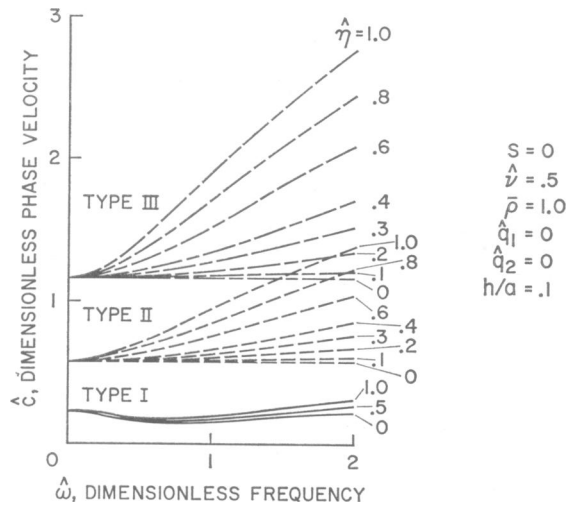

FIGURE 2 Dispersion curves of axisymmetric type I, II, and III waves for various values of the dimensionless viscosity coefficient of the vessel wall. Transmural pressure and axial stretch are both equal to zero.

For each circumferential wave number s, we find infinitely many waves with individual speeds of propagation. Within the parameter ranges pertaining to physiological problems all but the three slowest waves of each infinite set of waves for a given s are a direct consequence of the compressibility of the fluid. The results given as graphs in Figs. 2–28 are based on $c_f = 1500$ m/sec and are in agreement within the drawing accuracy with the results for an incompressible fluid ($c_f = \infty$). We shall identify the three slowest waves as waves of type I, II, and III. In waves of type I the radial displacement component is dominant at high frequencies, while

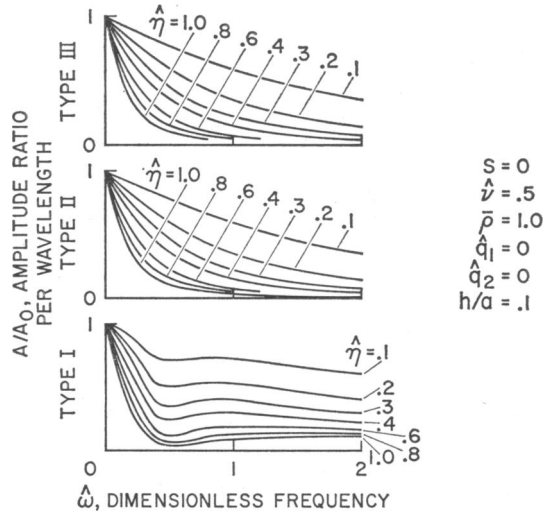

FIGURE 3 Amplitude ratio curves of axisymmetric type I, II, and III waves for various values of the dimensionless viscosity coefficient of the vessel wall. Transmural pressure and axial stretch are both equal to zero.

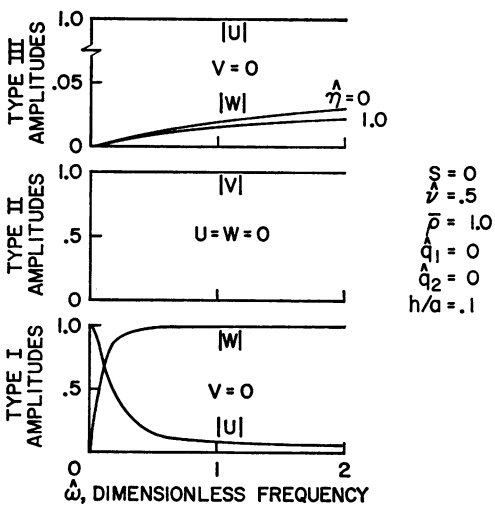

FIGURE 4 Mode shapes of axisymmetric type I, II, and III waves for various values of the dimensionless viscosity coefficient of the vessel wall. Transmural pressure and axial stretch are both equal to zero.

in waves of type II, the circumferential, and in waves of type III, the axial displacement components dominate at high frequencies. All of the faster waves exhibit cut-off frequencies (frequencies at which the phase velocity is infinite) and are transmitted only at frequencies above 1000 cycles/sec for physiologically meaningful parameter values. In this investigation we shall disregard these waves and consider only waves of type I, II, and III.

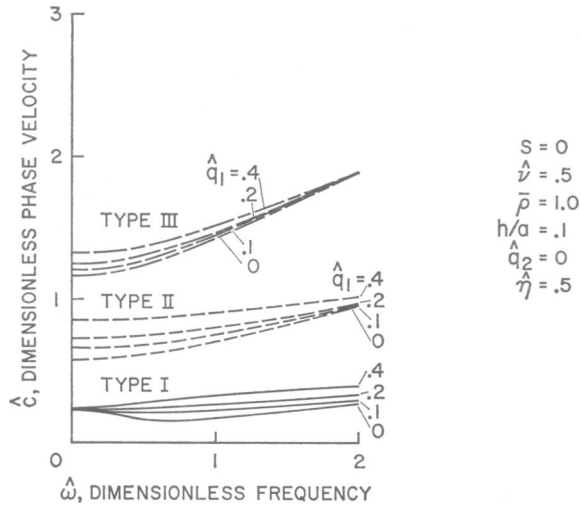

FIGURE 5 Dispersion curves of axisymmetric type I, II, and III waves for various axial stretches, zero transmural pressure, and dimensionless wall viscosity coefficient $\hat{\eta} = 0.5$.

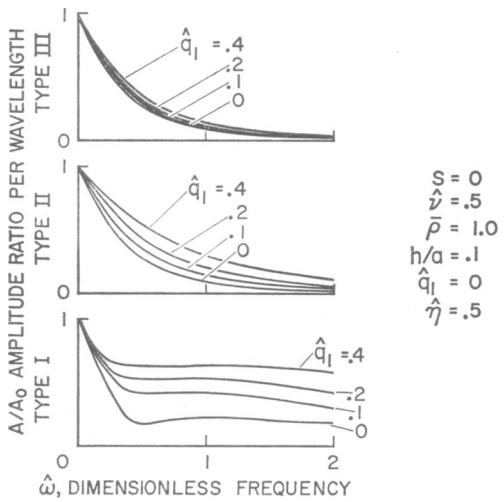

FIGURE 6 Amplitude ratio curves of axisymmetric type I, II, and III waves for various axial stretches, zero transmural pressure, and dimensionless wall viscosity coefficient $\hat{\eta} = 0.5$.

Discussion of Axisymmetric Waves

Fig. 2 presents the nondimensional axial phase velocity $\hat{c}$ for axisymmetric waves as a function of the nondimensional viscosity coefficient $\hat{\eta}$ ranging from 0 (elastic case) to 1.0. It should be recalled that type I waves have a displacement pattern that is predominantly radial in nature and therefore have associated with them considerably stronger pressure fluctuations than waves of type II and III. We note that as $\hat{\omega}$ approaches zero, the phase velocity of each of the three types of waves approaches

a limiting value which is independent of $\hat{\eta}$ and which is identical with the limiting value obtained in the elastic case.

For $\hat{\eta}\hat{\omega} \ll 1$ and $(h/a) \ll 1$ we can determine the phase velocities of type I waves approximately from

$$\hat{c}^2 \approx \frac{1}{(1-\hat{\nu}^2)} \frac{\left[h/2\bar{\rho}a + \hat{\nu}^2/\left(1 - 2\bar{\rho}\,\frac{a}{h}\right)\right]}{[(1 + 3\hat{\eta}^2\hat{\omega}^2)^{1/2} + 1]}. \tag{48}$$

From this it follows immediately that at very low frequencies, the effect of visco-

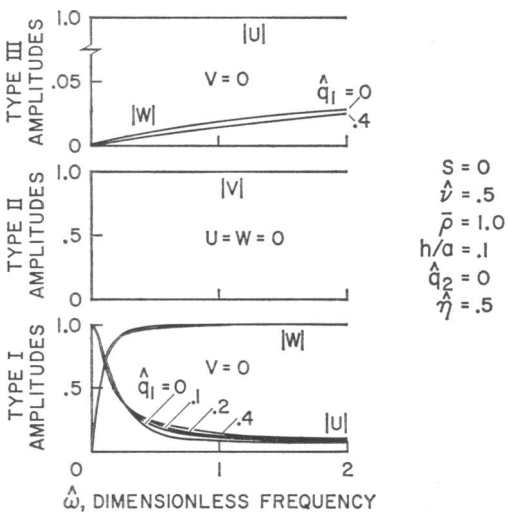

FIGURE 7 Mode shapes of axisymmetric type I, II, and III waves for various axial stretches, zero transmural pressure, and dimensionless wall viscosity coefficient $\hat{\eta}$ = 0.5.

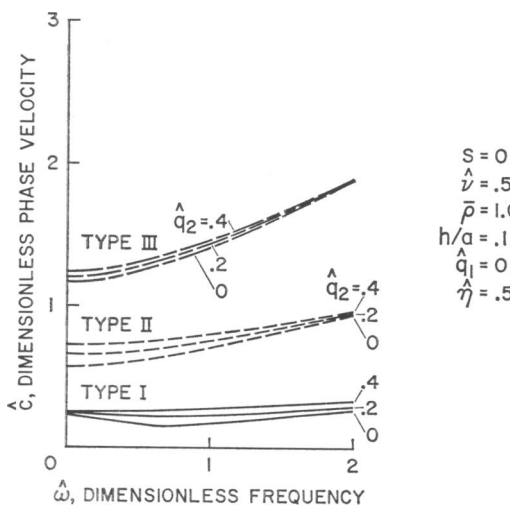

FIGURE 8 Dispersion curves of axisymmetric type I, II, and III waves for various transmural pressures, zero axial stretch, and dimensionless wall viscosity coefficient $\hat{\eta}$ = 0.5.

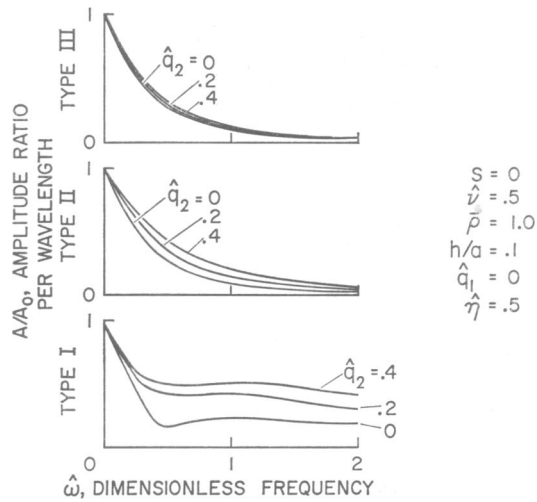

FIGURE 9 Amplitude ratio curves of axisymmetric type I, II, and III waves for various transmural pressures, zero axial stretch, and dimensionless wall viscosity coefficient $\hat{\eta} = 0.5$.

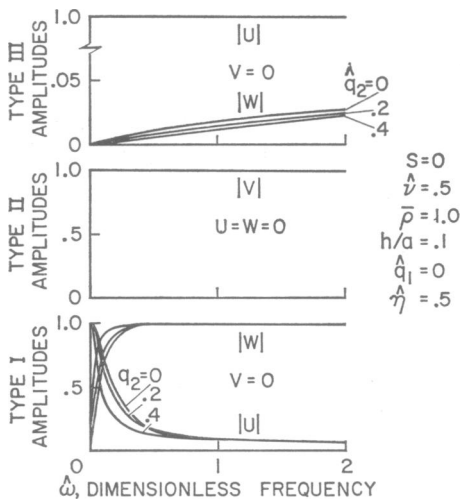

FIGURE 10 Mode shapes of axisymmetric type I, II, and III waves for various transmural pressures, zero axial stretch, and dimensionless wall viscosity coefficient $\hat{\eta} = 0.5$.

elasticity on dispersion of axisymmetric waves in a thin-walled vessel is only of second order. This result is of particular significance since it predicts that the viscoelastic behavior of blood vessels will practically have no effect on the phase velocities at low frequencies. Therefore, one cannot expect to determine reliably the viscoelastic parameters of blood vessels on the basis of phase velocity measurements of pressure waves.

The frequency equation yields an exact expression for the phase velocities of type II waves, which can be written in the form

$$\hat{c}^2 = \frac{(1 + 3e^2)}{(1 + \hat{\nu})} \frac{(1 + 3\hat{\eta}^2\hat{\omega}^2)}{[(1 + 3\hat{\eta}^2\hat{\omega}^2)^{1/2} + 1]}. \tag{49}$$

For type III waves, no closed form expression can be given for the phase velocities. However, with the restriction $\hat{\eta}\hat{\omega} \ll 1$ we find approximately for the speeds of axisymmetric type III waves

$$\hat{c}^2 \approx \frac{1}{(1 - \hat{\nu}^2)} \frac{\left[1 - \hat{\nu}^2/\left(1 - 2\bar{p}\,\frac{a}{h}\right)\right]}{[(1 + 3\hat{\eta}^2\hat{\omega}^2)^{1/2} + 1]}. \tag{50}$$

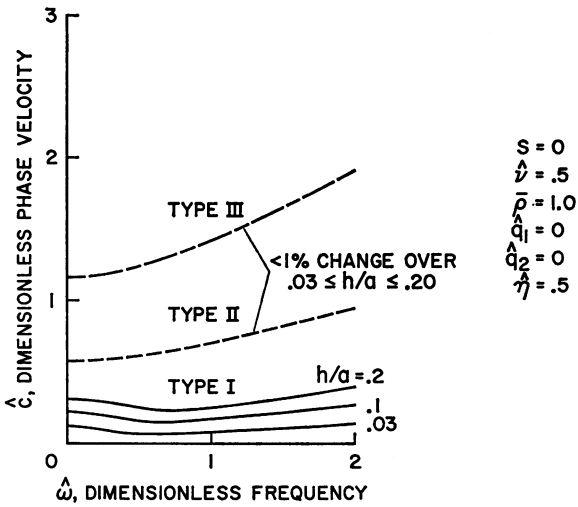

FIGURE 11 Dispersion curves of axisymmetric type I, II, and III waves for various wall thickness to radius ratios at zero transmural pressure, zero axial stretch, and dimensionless wall viscosity coefficient $\hat{\eta} = 0.5$.

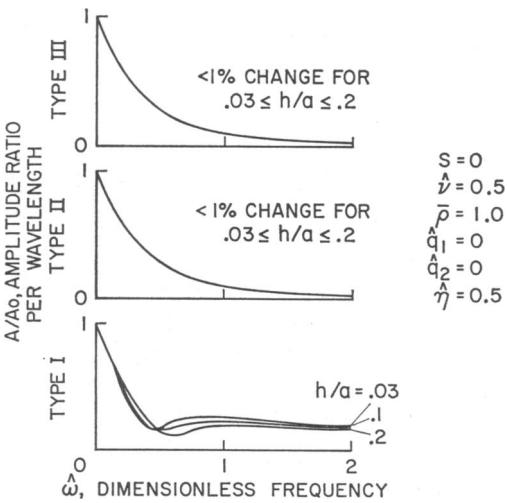

FIGURE 12 Amplitude ratio curves of axisymmetric type I, II, and III waves for various wall thickness to radius ratios at zero transmural pressure, zero axial stretch, and dimensionless wall viscosity coefficient $\hat{\eta} = 0.5$.

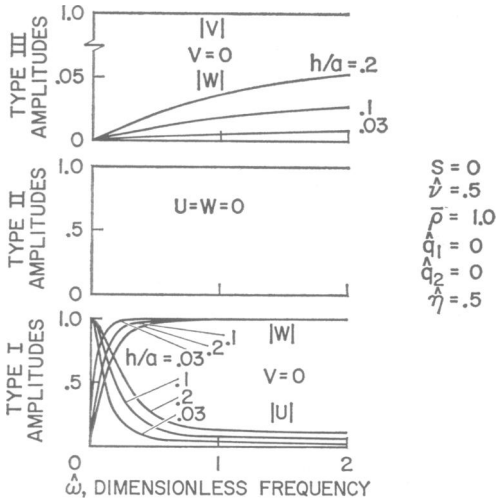

FIGURE 13 Mode shapes of axisymmetric type I, II, and III waves for various wall thickness to radius ratios at zero transmural pressure, zero axial stretch, and dimensionless wall viscosity coefficient $\hat{\eta} = 0.5$.

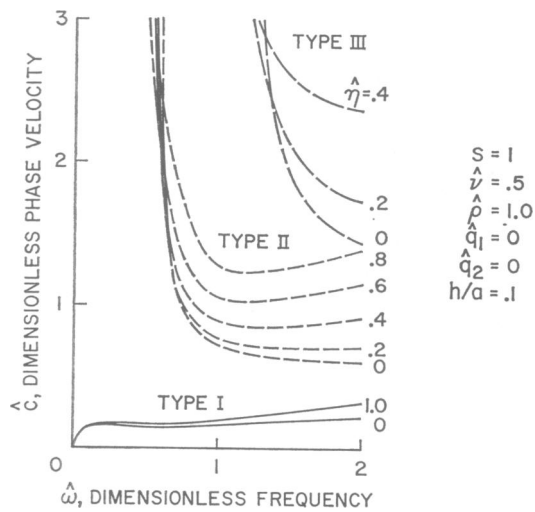

FIGURE 14 Dispersion curves of nonaxisymmetric ($s = 1$) type I, II, and III waves for various values of the dimension less viscosity coefficient of the yessel wall. Transmural pressure and axial stretch are both equal to zero. Below the elastic cut-off frequencies, $\hat{c} > 3.0$ for type II and III waves.

As can be seen from Fig. 2, type II and III waves become highly dispersive as $\hat{\eta}$ is increased from 0.0 to 1.0, although equations 49 and 50 indicate that the dispersion will be only of second order for small $\hat{\eta}\hat{\omega}$.

Fig. 3 depicts the damping per wavelength of axisymmetric waves as a function of the frequency parameter $\hat{\omega}$ for $0.0 \leqq \hat{\eta} \leqq 1.0$. In the case of type I waves, the curves indicate that for $\hat{\omega} \geqq 0.4$, the damping ratio A_λ/A_0 is essentially independent of frequency, for all values of $\hat{\eta} \leqq 1.0$. This property lends support to the appropriateness of the Voigt solid in shear as a model for the viscoelastic behavior of the vessel wall, since recent wave propagation experiments in the thoracic and abdominal aorta of anesthetized dogs have exhibited similar damping characteristics (11).

In this connection it should be emphasized that the experimental data referred to here includes the contribution of blood viscosity and radiation of energy into the vascular bed to the attenuation of waves in addition to the dissipation in the wall due to its viscoelasticity. A comparison of our theoretical results with experimental data from reference 11 suggests that $\hat{\eta}$ is less than 0.5 over the frequency range of 50 to 200 cycles per sec. This contrasts with $\hat{\eta} \approx 5$ implied by reference 15 for low frequency waves in the abdominal aorta of dogs.

At very low frequencies type II and type III waves are not as heavily damped as those of type I but are more heavily damped when $\hat{\omega} \geqq 0.4$. For waves of type II,

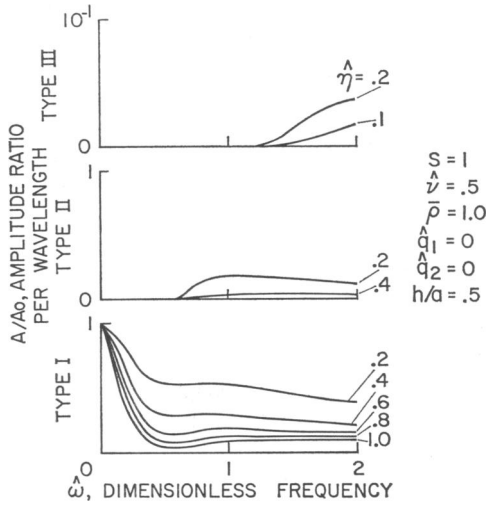

FIGURE 15 Amplitude ratio curves of nonaxisymmetric ($s = 1$) type I, II, and III waves for various values of the dimensionless viscosity coefficient of the vessel wall. Transmural pressure and axial stretch are both equal to zero.

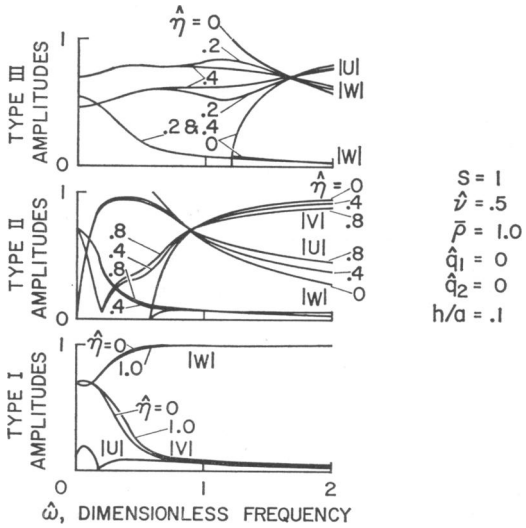

FIGURE 16 Mode shapes of nonaxisymmetric ($s = 1$) type I, II, and III waves for various values of the dimensionless viscosity coefficient of the vessel wall. Transmural pressure and axial stretch are both equal to zero.

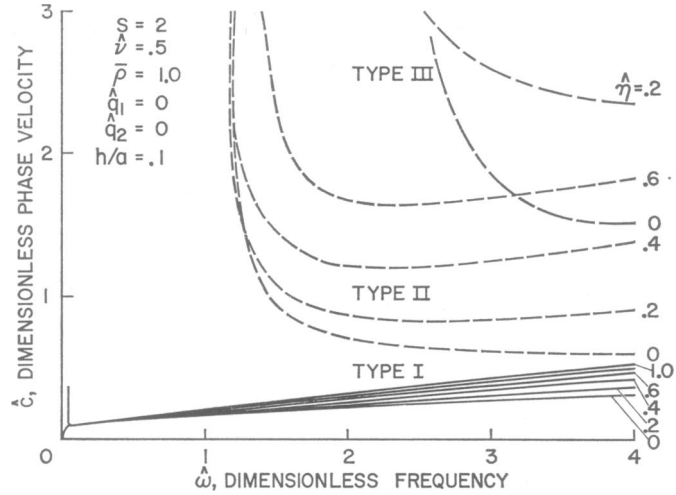

FIGURE 17 Dispersion curves of nonaxisymmetric ($s = 2$) type I, II, and III waves for various values of the dimensionless viscosity coefficient of the vessel wall. Transmural pressure and axial stretch are both equal to zero. Below the elastic cut-off frequencies, $\hat{c} > 3.0$ for type II and III waves.

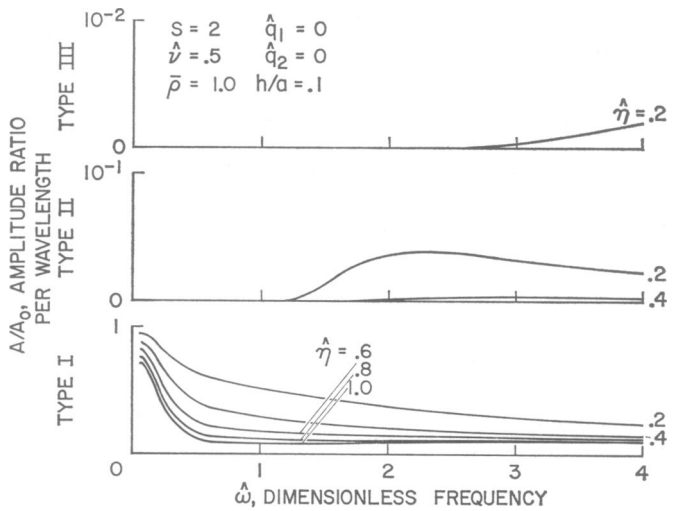

FIGURE 18 Amplitude ratio curves of nonaxisymmetric ($s = 2$) type I, II, and III waves for various values of the dimensionless viscosity coefficient of the vessel wall. Transmural pressure and axial stretch are both equal to zero.

the amplitude ratio A_λ/A_0 can be given in closed form as

$$\frac{A_\lambda}{A_0} = \exp\left\{-2\pi\left[\frac{(1 + 3\hat{\eta}^2\hat{\omega}^2)^{1/2} - 1}{(1 + 3\hat{\eta}^2\hat{\omega}^2)^{1/2} + 1}\right]^{1/2}\right\}. \tag{51}$$

No such closed form expression for A_λ/A_0 can be given for type I and III waves.

However, when $\hat{\eta}\hat{\omega} \ll 1.0$, the damping ratio for all three types can be approximated by

$$\frac{A_\lambda}{A_0} \approx \exp\left(-\sqrt{3\pi\hat{\eta}\hat{\omega}}\right) \approx 1 - \sqrt{3\pi\hat{\eta}\hat{\omega}}. \tag{52}$$

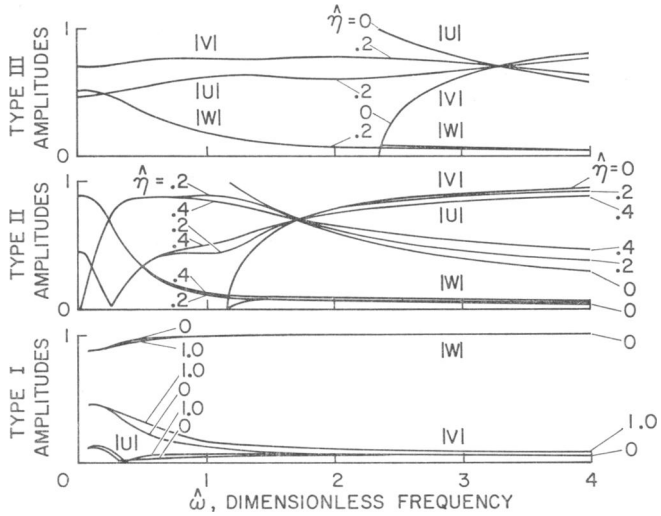

FIGURE 19 Mode shapes of nonaxisymmetric ($s = 2$) type I, II, and III waves for various values of the dimensionless viscosity coefficient of the vessel wall. Transmural pressure and axial stretch are both equal to zero, with $h/a = 0.1$, $\bar{\rho} = 1.0$, and $\hat{\nu} = 0.5$.

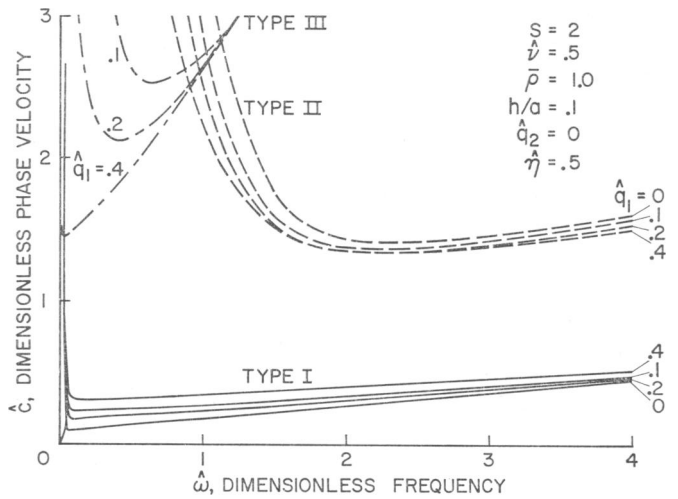

FIGURE 20 Dispersion curves of nonaxisymmetric ($s = 2$) type I, II, and III waves for various axial stretches, zero transmural pressure, and dimensionless wall viscosity coefficient $\hat{\eta} = 0.5$. Below the elastic cut-off frequencies, $\hat{c} > 3.0$ for type II waves.

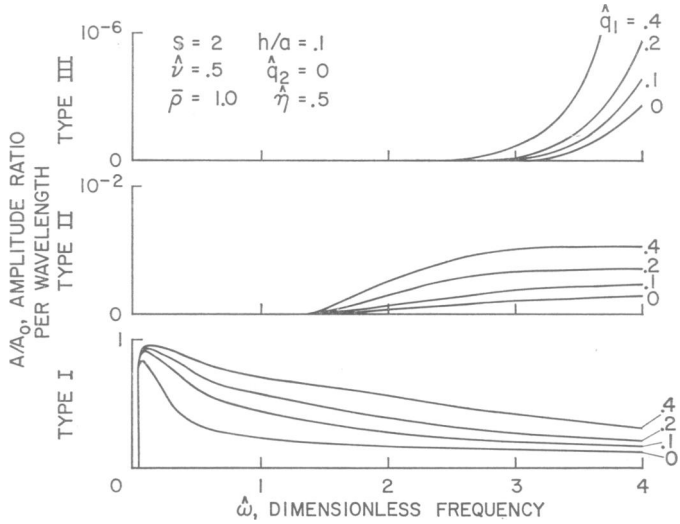

FIGURE 21 Amplitude ratio curves of nonaxisymmetric ($s = 2$) type I, II, and III waves for various axial stretches, zero transmural pressure, and dimensionless wall viscosity coefficient $\hat{\eta} = 0.5$.

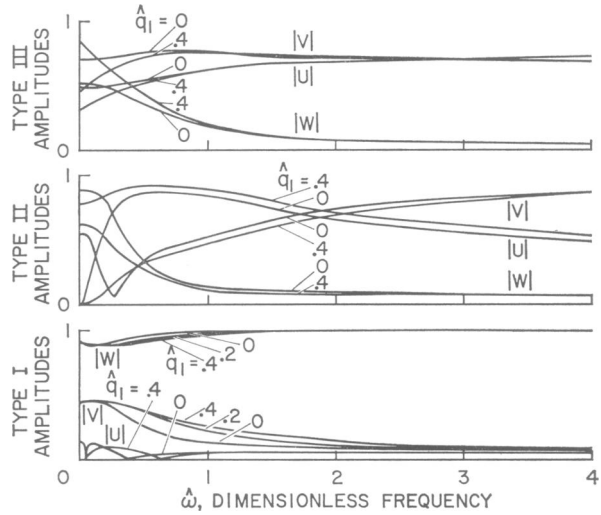

FIGURE 22 Mode shapes of nonaxisymmetric ($s = 2$) type I, II, and III waves for various axial stretches, zero transmural pressure, and dimensionless wall viscosity coefficient $\hat{\eta} = 0.5$, with $h/a = 0.1$, $\bar{\rho} = 1.0$, and $\hat{\nu} = 0.5$.

From equation 52 we conclude that, for small $\hat{\eta}\hat{\omega}$, the damping ratio decreases linearly with $\hat{\eta}$ or $\hat{\omega}$.

The mode shapes for axisymmetric waves are nearly independent of $\hat{\eta}$ for $\hat{\eta} \leqq 1.0$, as is evident from Fig. 4. Only the radial components of type III waves show any

noticeable change with $\hat{\eta}$. Changes in the type I mode shapes are so small as to fall within the plotting accuracy of the curves.

Fig. 5 depicts the phase velocities of axisymmetric type I, II, and III waves for $\hat{\eta} = 0.5$ and for four values of the axial stretch parameter $\hat{q}_1$. While dispersion of type I waves due to axial stretch is only significant at higher frequencies, we find

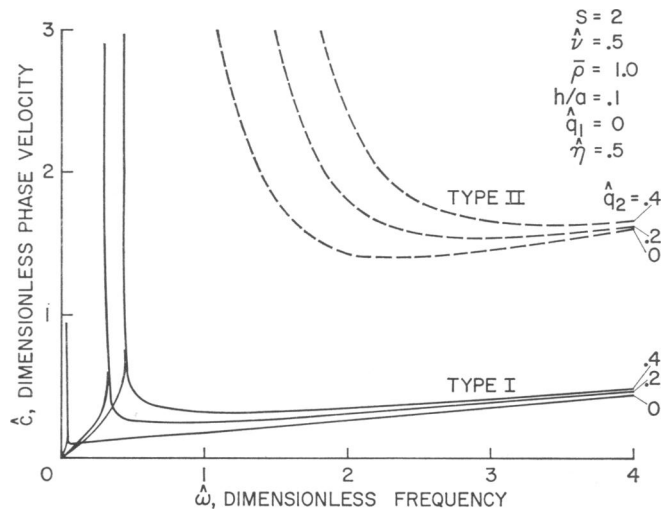

FIGURE 23 Dispersion curves of nonaxisymmetric ($s = 2$) type I, II, and III waves for various transmural pressures, zero axial stretch, and dimensionless wall viscosity coefficient $\hat{\eta} = 0.5$. Below the elastic cut-off frequencies, $\hat{c} > 3.0$ for type II and III waves.

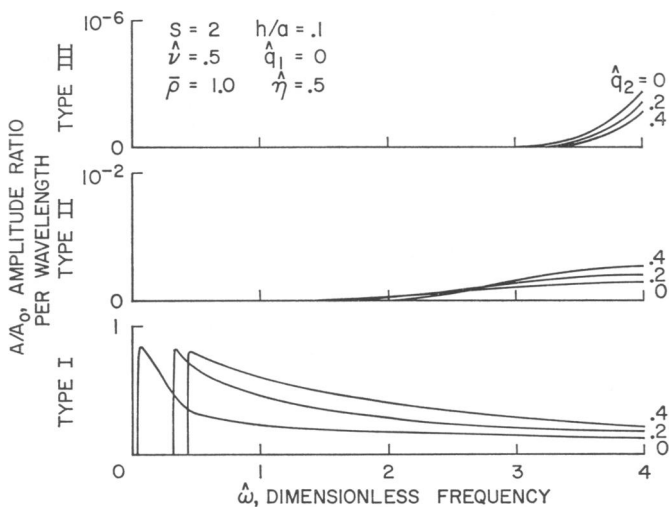

FIGURE 24 Amplitude ratio curves of nonaxisymmetric ($s = 2$) type I, II, and III waves for various transmural pressures, zero axial stretch, and dimensionless wall viscosity coefficient $\hat{\eta} = 0.5$.

that stretching affects the speed of waves of type II and III primarily at lower frequencies. From Fig. 6, it is seen that axial stretch has a marked effect on the magnitude of the damping of type I waves for $\hat{\eta} = 0.5$. When $\hat{q}_1 = 0.2$, the attenuation per wavelength at high frequencies is less than half of that for $\hat{q}_1 = 0$. This serves to emphasize that viscoelastic parameters extracted from data pertaining to high frequency pressure waves may be seriously in error if vessel stretch is not considered. The effect of axial stretch on the mode shapes of axisymmetric waves is negligible, as can be seen from Fig. 7.

The results of the effects of a transmural pressure on the dispersion, mode shapes, and attenuation of axisymmetric waves are illustrated in Figs. 8–10. We note that the effects on the wave propagation characteristics of a transmural pressure and an axial stretch are quite similar in nature. This is to be expected, since an axial stretch and a transmural pressure Δp both have in general a stiffening effect on the vessel.

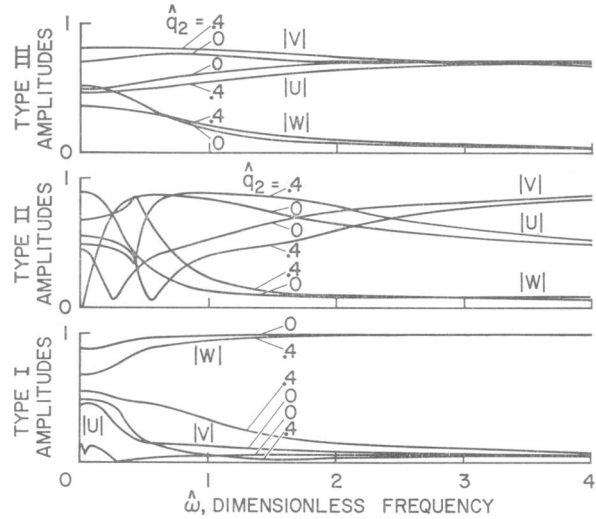

FIGURE 25 Mode shapes of nonaxisymmetric ($s = 2$) type I, II, and III waves for various transmural pressures, zero axial stretch, and dimensionless wall viscosity coefficient $\hat{\eta} = 0.5$, with $h/a = 0.1$, $\bar{\rho} = 1.0$, and $\hat{p} = 0.5$.

The thickness ratio h/a significantly affects the phase velocities of type I waves, as in the elastic case, but leaves the speed of type II and type III waves nearly unchanged, as can be seen from Fig. 11. According to Fig. 12, the damping ratio A_λ/A_0 is remarkably insensitive to variations in h/a for all three types of waves. Similarly, we find no significant changes in the mode shapes for different values of h/a as shown in Fig. 13.

Discussion of Nonaxisymmetric Waves

In the case of vessels with an elastic wall material, it was shown earlier that cut-off frequencies exist for nonaxisymmetric waves of types I, II, and III, with the sole

exception of type I waves with $s = 1$ (10). If the vessel wall is composed of an incompressible viscoelastic material, whose shear deformation is governed by the Voigt model, we no longer find cut-off frequencies in the classical sense. Nonaxisymmetric waves are now, theoretically, being propagated at all frequencies. However, as will be seen, the amplitude ratio A_λ/A_0 of waves propagating near and below the corresponding elastic cut-off frequency is so small that the experimental verification of their existence would be a question of sensitivity of the transducers utilized. For practical purposes one might therefore consider introducing a cut-off frequency on the basis of a minimal observable wave amplitude.

Discussion of Waves with $s = 1$

For $s = 1$, the phase velocities of type I waves exhibit only mild dispersion when $\hat{\alpha}$ varies between 0 and 1.0, as can be seen from Fig. 14. On the other hand, the

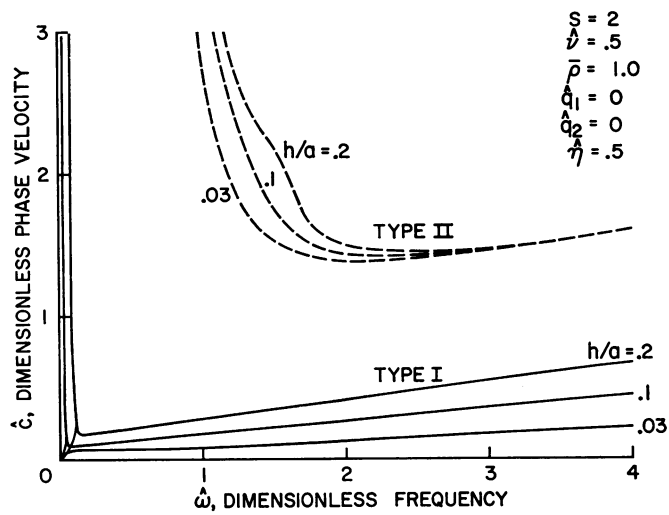

FIGURE 26 Dispersion curves of nonaxisymmetric ($s = 2$) type I, II, and III waves for various wall thickness to radius ratios at zero transmural pressure, zero axial stretch, and dimensionless wall viscosity coefficient $\hat{\eta} = 0.5$. Below the elastic cut-off frequencies, $\hat{c} > 3.0$ for type II and III waves.

speed of waves of type II and III are strongly dependent on $\hat{\eta}$ and $\hat{\omega}$. Except for $\hat{\eta} = 0$, cut-off frequencies no longer exist for type II and type III waves, although this is not readily apparent from Fig. 14. Considering, however, the variation of the mode shapes with frequency, as illustrated in Fig. 16, we note that waves are indeed being propagated below the elastic cut-off frequency for all values of $\hat{\eta}$ covered in our parametric study. We also see that the mode shape of type I waves is practically unaltered by increasing $\hat{\eta}$ from 0 to 1.0, while the type II and type III mode shapes exhibit great sensitivity to changes in $\hat{\eta}$.

According to Fig. 15, type I waves exhibit attenuation properties similar to those of axisymmetric type I waves, i.e. the attenuation per wavelength is again

essentially independent of frequency for $\hat{\omega} \gg 0.4$. In contrast to this, even comparatively small values of $\hat{\eta}$ lead to a strong attenuation per wavelength as compared with the axisymmetric case.

Discussion of Waves with $s = 2$

From the results given in Fig. 17, we again note that the speed of propagation of type I waves is only mildly affected by changes in $\hat{\eta}$ between 0 and 1.0. The phase velocities of type II and III waves on the other hand are strongly dependent on the viscoelasticity of the vessel wall. Propagation of all three types of waves below the elastic cut-off frequencies is again possible but damping per wavelength below cut-off is so high that they can be ignored, as is evident from Fig. 18.

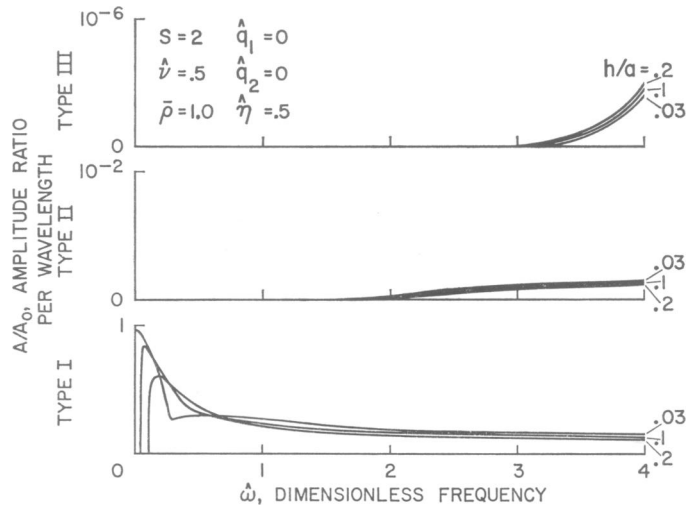

FIGURE 27 Amplitude ratio curves of nonaxisymmetric ($s = 2$) type I, II, and III waves for various wall thickness to radius ratios at zero transmural pressure, zero axial stretch, and dimensionless wall viscosity coefficient $\hat{\eta} = 0.5$.

From Fig. 19 it follows that type II and III mode shapes exhibit strong dependence on the parameter $\hat{\eta}$ for all $\hat{\omega} \leqq 4.0$, while the mode shape for $0 \leqq \hat{\eta} \leqq 1.0$ is indistinguishable from that of the elastic case ($\hat{\eta} = 0$).

Figs. 20–22 illustrate the sensitivity of both $\hat{c}$ and A_λ/A_0 to axial stretch when $\hat{\eta} = 0.5$. Near the elastic cut-off frequency, type I phase velocities may double in magnitude as $\hat{q}_1$ is increased from 0 to 0.2. Likewise, the amplitude ratio may grow by more than a factor of two with the same change in stretch. The sensitivity of the phase velocities and damping characteristics of type II and III waves to changes in axial stretch may be equally pronounced, but for practical purposes unimportant in view of the heavy damping. From Fig. 22, we see that mode shapes show no significant dependence on $\hat{q}_1$ except at low frequencies.

The effects of a transmural pressure on phase velocities, damping characteristics and mode shapes of $s = 2$ waves are summarized in Figs. 23–25 for $\hat{\eta} = 0.5$. The dispersive nature of these waves is essentially similar to that of the elastic case, except for the existence of waves below the elastic cut-off frequency. The amplitude ratio A_λ/A_0 of type I waves increases markedly with rising transmural pressure, while the absolute changes in the amplitude ratio of type II and III waves may be termed insignificant.

The results plotted in Figs. 26–28 illustrate the influence of changes in the thickness ratio h/a on the propagation characteristics of $s = 2$ waves for $\hat{\eta} = 0.5$. Variations in the thickness ratio have a strong influence on the phase velocities of waves of type I. Except near the elastic cut-off frequencies, the phase velocities of type I

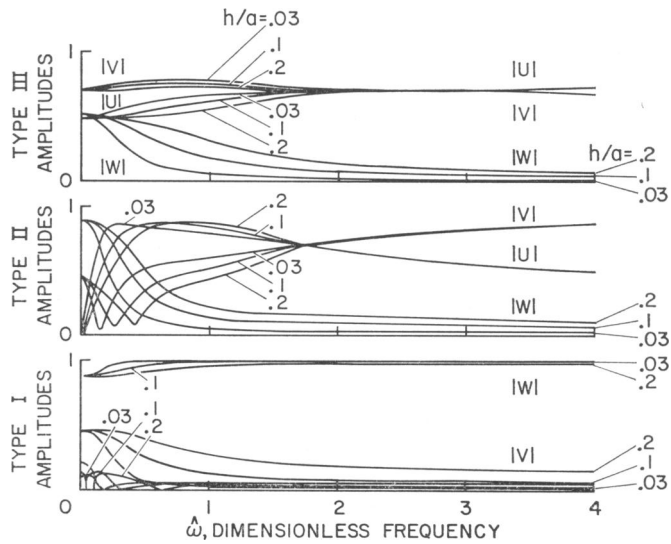

FIGURE 28 Mode shapes of nonaxisymmetric ($s = 2$) type I, II, and III waves for various wall thickness to radius ratios at zero transmural pressure, zero axial stretch, and dimensionless wall viscosity coefficient $\hat{\eta} = 0.5$, with $h/a = 0.1$, $\bar{\rho} = 1.0$, and $\hat{\nu} = 0.5$.

waves vary approximately as $(h/a)^{1/2}$. On the other hand, Figs. 27 and 28 demonstrate that the damping characteristics and mode shapes of such waves are only moderately affected by variations in h/a. Waves of type II and III show only unimportant changes in their characteristics with respect to changes in h/a except below the elastic cut-off frequencies. It becomes clear, however, from Fig. 27, that these changes are of no practical significance because of the severe damping.

CONCLUSIONS

From our dispersion curves we conclude that a realistic model for the dynamic behavior of blood vessels should include the effects of the transmural pressure and

the axial stretch. The propagation of pressure pulses similar to those generated by the heart appears to involve primarily axisymmetric waves of type I since waves of type II are not connected with intraluminal pressure fluctuations and waves of type III exhibit only very small pressure perturbations. Qualitative agreement is obtained with recent experiments on dissipation of high frequency waves in blood vessels by assuming that the vessel wall material is incompressible but behaves as a Voigt solid in shear. The phase velocities of type I axisymmetric waves are only mildly affected by such viscoelastic behavior, so that it will be difficult to obtain accurate estimates of the viscoelastic parameters of the vessel wall on the basis of type I phase velocity measurements only. The dissipation of waves, however, exhibits a strong dependence on the viscoelastic properties of the vessel wall. Moreover, the dissipation decreases substantially with increasing axial stretch or transmural pressure, especially at high frequencies. Consequently, the reliable determination of the viscoelasticity of the vessel wall from experiments involving high frequency wave propagation must take into consideration the effects of axial stretch and transmural pressure. Considering the striking dispersive properties of nonaxisymmetric waves, their experimental verification would offer deeper insight into the viscoelastic behavior of arteries and veins. The effects of the compressibility of the blood are insignificant for waves with frequencies below 1000 cycles per sec.

This work was performed at Stanford University and at the Ames Research Center of the NASA with the sponsorship of the U. S. Army Research Office under Contract No. DA-31-124-ARO-D-223, the National Science Foundation under Grant No. GK-47 and the NASA under Grant No. NGR-05-020-223.

Received for publication 17 January 1968.

NOMENCLATURE

a	Equilibrium radius of the middle surface of the vessel wall.
A_λ	Wave amplitude at a distance of 1 wavelength from origin.
A_0	Wave amplitude at origin.
A_{sk}, B_{sk}, C_{sk}	Mode amplitudes for circumferential wave number s, axial wave number ka.
c	ω/k_R = axial phase velocity.
c_b	$(3E_0/\rho_w)^{1/2}$ = normalizing phase velocity (viscoelastic shell).
c_f	Speed of sound in blood.
c_p	$[E/\rho_w(1 - \nu^2)]^{1/2}$ = normalizing phase velocity (elastic shell).
$\bar{c}$	c/c_p = dimensionless phase velocity (elastic shell).
$\hat{c}$	c/c_b = dimensionless phase velocity (viscoelastic shell).
c^*	c_f/c_p = dimensionless speed of sound in blood (elastic shell).
$\hat{c}^*$	c_f/c_b = dimensionless speed of sound in blood (viscoelastic shell).
D	$\partial/\partial t$ = differential operator.
D_{sk}	Constant related to initial conditions of fluid.
e^2	$h^2/(12a^2)$ = dimensionless parameter.
E	Young's modulus of vessel wall.
E_0	Zero frequency modulus, viscoelastic shell.

$\hat{E}$	Complex Young's modulus.
G	Elastic shear modulus.
h	Thickness of vessel wall.
i	$(-1)^{1/2}$
$I_s(\xi)$	Modified Bessel function of the first kind, argument ξ.
ka	$(k_R + ik_I)a$ = complex axial wave number.
k_R	$Re(ka/a)$
k_I	$Im(ka/a)$
K	Elastic bulk modulus.
L_{ij}	Differential operators.
m_f	Radial apparent mass of blood contained in the vessel.
p_e	External pressure applied to vessel.
p_i	Perturbed internal pressure applied to vessel.
p_{io}	Unperturbed internal pressure.
P, P'	Viscoelastic operators.
q_1	$T_{10}(1 - \nu^2)/Eh$ = dimensionless axial stress resultant.
q_2	$a\Delta p(1 - \nu^2)/Eh$ = dimensionless radial stress resultant.
$\hat{q}_1$	$T_{10}/(3E_0h)$ = dimensionless axial stress resultant (viscoelastic shell).
$\hat{q}_2$	$a\Delta p/(3E_0h)$ = dimensionless radial stress resultant (viscoelastic shell).
Q, Q'	Viscoelastic operators.
r	Coordinate in radial direction.
s	Circumferential wave number.
t	Time.
T_{10}	Initial axial tension of vessel.
u, v, w	Displacements of vessel middle surface in axial, circumferential, and radial directions respectively.
$\mathbf{v}$	Fluid velocity.
x	Coordinate in axial direction.
α	x/a = dimensionless axial coordinate.
β	Coordinate in circumferential direction.
Δp	$p_{io} - p_e$ = transmural pressure.
η	Vessel wall coefficient of viscosity.
$\hat{\eta}$	$\eta/[a\rho_w(E_0/\rho_w)^{1/2}]$ = dimensionless vessel wall coefficient of viscosity.
μ_f	Fluid inertia parameter.
μ_w	$(1 - \nu^2)a^2(\rho_w h)/Eh$ = wall inertia parameter.
ν	Poisson's ratio.
$\hat{\nu}$	Complex Poisson's ratio (viscoelastic shell).
$\bar{\rho}$	ρ_f/ρ_w = dimensionless density ratio.
ρ_f	Blood density.
ρ_w	Vessel wall density.
Φ	Fluid velocity potential.
ξ	$\left(k^2a^2 - \frac{\omega^2a^2}{c_f^2}\right)^{1/2}$ = dimensionless parameter.
ω	Angular frequency.
$\bar{\omega}$	$\omega a/c_p$ = dimensionless angular frequency (elastic shell).
$\hat{\omega}$	$\omega a/c_b$ = dimensionless angular frequency (viscoelastic shell).
∇	Gradient operator.
∇^2	Laplacian operator.

REFERENCES

1. McDONALD, D. A. 1960. Blood Flow in Arteries. Edward Arnold, Ltd., London, England.
2. FOX, E. A., and EDWARD SAIBEL. 1963. *Trans. Soc. Rheol.* **7**:25.
3. KLIP, WILLEM. 1962. Velocity and Damping of the Pulse Wave. Martinus Nijhoff, The Hague, The Netherlands.
4. WOMERSLEY, J. R. 1957. An Elastic Tube Theory of Pulse Transmission and Oscillatory Flow in Mammalian Arteries. WADC Tech. Rept. TR 56-614. Wright Air Development Center, Ohio.
5. ATTINGER, E. O., editor. 1964. Pulsatile Blood Flow: Proceedings. Blakiston Div., McGraw-Hill Book Co., New York.
6. LIN, T. C., and G. W. MORGAN. 1956. *J. Acoust. Soc. Am.* **28**:1165.
7. ANLIKER, MAX, and K. R. RAMAN. 1966. *Intern. J. Solids Struct.* **2**:467.
8. FLÜGGE, W. 1962. Stresses in Shells. Springer-Verlag, Berlin, Germany.
9. ATABEK, H. B., and H. S. LEW. 1966. *Biophys. J.* **6**:481.
10. ANLIKER, MAX, and J. A. MAXWELL. 1966. The dispersion of waves in blood vessels. Proc. Am. Soc. Mech. Engr. Symp. Biomech. New York.
11. ANLIKER, MAX, M. HISTAND, E. OGDEN, and R. M. WESTBROOK. 1966. Direct measurement of dissipation of waves in arteries and veins. *Proc. Ann. Conf. Eng. Med. Biol.* **8**: 17.
12. JONES, E. 1966. Oscillatory, axially symmetric motion of an elastic tube containing a streaming Newtonian fluid. Proc. 1966 Divisional Meeting Division of Fluid Dynamics. American Physical Society, Stanford, Calif.
13. JONES, E. 1968. Effects of viscosity and external constraints on wave transmission in blood vessels. Ph.D. dissertation. Department of Aeronautics and Astronautics, Stanford University, Stanford, Calif.
14. BERGEL, D. H. 1961. *J. Physiol. (London)* **156**:458.
15. McDONALD, D. A., and URS GESSNER. 1966. Wave attenuation in viscoelastic arteries. Proc. First Intern. Conf. Hemorheology. Pergamon Press, Oxford, England.
16. HARDUNG, V. 1962. *In* Handbook of Physiology, Circulation. American Physiological Society, Washington, D. C. **1**:107.
17. GREENSPON, J. E. 1961. *J. Acoust. Soc. Am.* **33**:1321.